

# Structural, thermal and micro-mechanical properties of Polyvinyl butyral (PVB) and Poly (vinylidene fluoride-co-Hexafluoropropylene) (PVDF-HFP) blends

Manjula Bhumarkar<sup>1</sup>, Swarnim Patel<sup>2\*</sup>, Purvee Bhardwaj<sup>3</sup>

<sup>1,3</sup>Department of Physical Science, Rabindranath Tagore University, Raisen, M.P., India (464993).

<sup>2\*</sup>Govt. College Amarpur, Dindori, M.P., India (481880)

\*Corresponding author: Swarnim Patel

\*swarnimpatel17@gmail.com

**Abstract**-This paper focuses on the structural, mechanical, and micro-hardness properties of PVB: PVDF-HFP blends. These blends were prepared using the solution casting technique. The prepared blend samples were analyzed using Fourier Transform Infrared (FT-IR) spectroscopy, X-ray diffraction (XRD), Differential Scanning Calorimetry (DSC) and microhardness testing. The FT-IR and XRD spectra of pure PVB, pure PVDF-HFP, and their blends were observed and analyzed. The analysis confirmed the molecular interaction between the two polymers and the dominant presence of the  $\alpha$ -phase of PVDF-HFP in the blends. X-ray diffraction was used to investigate the crystalline size, revealing that the crystallinity index increases with the concentration of PVDF-HFP in the blend. The DSC study focused on the glass transition range of the blends, indicating that they have a single glass transition temperature, suggesting miscibility/ or compatibility in the selected composition range. The Vickers microhardness indentation technique was used to assess the effect of PVDF-HFP on PVB. Various characterizations in this study indicate that the prepared blends are compatible within the selected composition range.

**Keywords:** PVB, PVDF-HFP, FTIR,  $\alpha$ -phase, DSC

## 1. INTRODUCTION

Polymer blends have garnered significant attention in materials science and engineering due to their ability to combine the desirable properties of different polymers into a single material. Among various polymer blends, the combination of polyvinyl butyral (PVB) and poly (vinylidene fluoride-co-hexafluoropropylene) (PVDF-HFP) stands out for its potential in numerous applications, ranging from flexible electronics to high-performance coatings [1]. This paper focuses on the structural, thermal, and micro-mechanical properties of PVB and PVDF-HFP blends, highlighting their potential for advanced material applications.

Polyvinyl butyral (PVB) is a well-known polymer primarily used in safety glass laminates due to its excellent adhesive properties, transparency, and flexibility. PVB's characteristics make it an ideal candidate for blending with other polymers to enhance its mechanical and thermal properties [2]. On the other hand, PVDF-HFP, a copolymer of vinylidene fluoride and hexafluoropropylene, is renowned for its outstanding chemical resistance, thermal stability, and ferroelectric properties [3]. The combination of PVB and PVDF-HFP could potentially result in a material that harnesses the beneficial properties of both polymers, such as improved mechanical strength, thermal stability, and enhanced microhardness.

The primary objective of this study is to investigate the structural, thermal, and micro-mechanical properties of PVB: PVDF-HFP blends. The research aims to understand the interactions between PVB and PVDF-HFP at the molecular level and how these interactions influence the overall properties of the blends.

Previous studies have explored various aspects of PVB and PVDF-HFP individually [1-3], but comprehensive studies on their blends are relatively scarce. PVB has been extensively studied for its applications in laminated safety glass, where its mechanical and adhesive properties are critical. Studies have shown that PVB exhibits good flexibility and impact resistance, making it suitable for various applications beyond safety glass.

PVDF-HFP has been widely investigated for its use in high-performance applications, including piezoelectric devices, chemical-resistant coatings, and membranes for fuel cells. The unique properties of PVDF-HFP, such as its ferroelectricity and high thermal stability, make it an attractive candidate for blending with other polymers to create materials with enhanced properties [2].

Combining PVB with PVDF-HFP could result in a blend that benefits from the advantageous properties of both polymers. However, the exact nature of the interaction between these two polymers and its effect on the overall properties of the blend remains an area that requires thorough investigation.

The study aims to provide a comprehensive understanding of the structural, thermal, and micro-mechanical properties of PVB: PVDF-HFP blends. By elucidating the interactions between PVB and PVDF-HFP, the research is expected to reveal how these blends can be tailored for specific applications. The insights gained from this study could lead to the development of new materials with improved performance characteristics, potentially impacting various industries, including electronics, coatings, and automotive sectors.

## 2. MATERIALS AND METHOD

The commercial PVB and PVDF-HFP powders utilized in this study were obtained from Merck, India and distributed by Sameer Science Lab, India. These polymers and chemicals were used as received, with no further purification.

The samples for this study were prepared using the solution casting technique [4]. Specified concentrations of solutions were created by dissolving the PVB and PVDF-HFP polymers in varying weight ratios in N,N-Dimethylformamide (DMF) at 80°C. Blend samples, each measuring 6 cm<sup>2</sup> with a thickness of approximately 20±5 µm, and with PVB: PVDF-HFP weight compositions of 100:0; 95:05; 90:10; 85:15; 80:20; 85:15; and 0:100, were prepared

### 2.1 FT-IR Analysis

The FT-IR spectra of the samples were obtained using a Shimadzu FTIR-8400 spectrophotometer. Spectra were recorded in the range of 4000 to 500 cm<sup>-1</sup>. Each spectrum was captured with a resolution of 2 cm<sup>-1</sup> over 25 cumulative scans by mounting a film of the appropriate dimensions on the sample holder in transmission mode.

### 2.2 XRD Analysis

X-ray diffraction patterns were employed to observe changes in the crystalline and amorphous regions of the samples. The specimens were positioned in an aluminum sample holder, exposing the upper smooth surface to X-rays in a vertical goniometer assembly. The scanning was conducted over a range of 3 to 60° at a speed of 4°/min, with an operating voltage of 40 kV and a current of 15 mA. CuKα radiation, with a wavelength of 1.540 Å, was utilized on a Rigaku Miniflex 600 Benchtop Powder X-Ray Diffraction (XRD) Instrument.

### 2.3 DSC Analysis

The glass transition temperature of the blend samples was characterized using a DSC-60 Plus Series Differential Scanning Calorimeter. The calorimeter employed a heat flux measurement type and operated over a temperature range from -140°C to 600°C. The analysis was conducted in the temperature range of 0°C to 300°C at a heating rate of 10°C/min. To achieve the necessary low temperatures for analysis, liquid nitrogen was utilized.

### 2.4 Microhardness measurements

Microhardness measurements on various specimens were performed using an MPH 160 microhardness tester equipped with a Vickers diamond pyramidal indenter attached to a Carl Zeiss NU2 universal research microscope. The Vickers hardness number (HV) was calculated using the following relation:

$$H_v = \frac{1.854 * L}{d^2} \text{ Kg/mm}^2$$

where L is the load in kg and d is the diagonal of the indentation in mm. Multiple indentations were made at various loads, and the average hardness number was calculated.

## 3. RESULTS AND DISCUSSION

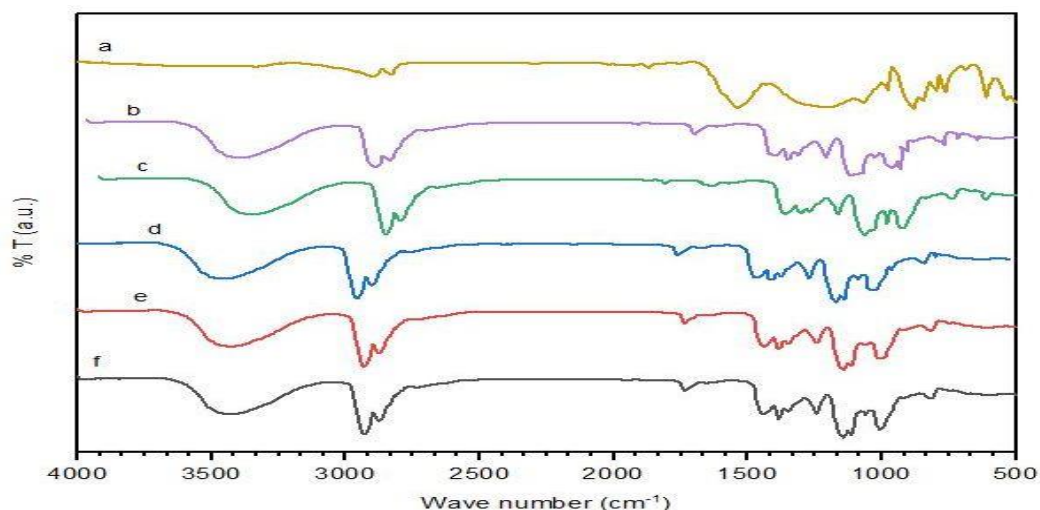
### 3.1 FT-IR

Figure 1 illustrates the FT-IR spectra of pure PVB and PVDF-HFP, as well as their blend samples at weight ratios of PVB:PVDF-HFP 95:05, 90:10, 85:15, and 80:20. These spectra were analyzed to identify characteristic bands of the individual polymers and any interactions present in the blends [5-7].

In the FT-IR spectra of the blend samples, typical peaks associated with pure PVB and PVDF-HFP were observed. Shifts in characteristic bands related to functional groups such as -OH, -CF<sub>2</sub>, and -CF from their positions in the pure polymers suggest chemical interactions between the two [8]. Additionally, distinct absorption bands were noted in the fingerprint regions.

As the weight percentage of PVDF-HFP increased in the blends, there was a noticeable shift in absorption bands and a decrease in transmittance, indicating miscibility and compatibility within the studied composition range. Characteristic bands at 976, 843, 795, 610, and 532 cm<sup>-1</sup>, corresponding to the α-phase of PVDF-HFP, were also present in the blend samples [9]. These bands became more prominent with higher PVDF-HFP content, suggesting an increase in crystallinity.

The samples were prepared using the solution casting technique with DMF as the solvent, at an evaporation temperature of 80°C. Under these conditions, the films obtained were predominantly in the alpha phase in their unpoled state [10].



**Figure 1:** FTIR plots of pure PVB, PVDF-HFP and their blends i.e. PVB: PVDF-HFP:: 95:05;90:10;85:15 and 80:20

### 3.2XRD

X-ray diffraction (XRD) patterns were obtained to analyze the crystalline, semi-crystalline, and amorphous characteristics of pure polymers and their blend samples. Figure 2 shows the XRD patterns of pure PVB, PVDF-HFP, and their blends. The XRD pattern of the pure PVB film exhibits an amorphous feature characterized by a halo centered at  $2\theta = 23.94^\circ$ . This halo pattern and peak positions are consistent with XRD patterns reported for PVB by various authors [2, 11], confirming that the PVB in this study remains in its amorphous state. The XRD pattern of the PVDF-HFP film shows an intense peak at  $2\theta = 19.68^\circ$ , with a shoulder peak at  $18.18^\circ$  and additional noticeable peaks at  $2\theta = 26.58^\circ$  and  $38.7^\circ$ . PVDF-HFP typically exists in multiple phases ( $\alpha$ ,  $\beta$ ,  $\gamma$ ,  $\delta$ ,  $\epsilon$ ) [12], and in this case, the peak positions indicate that PVDF-HFP is primarily in its  $\alpha$ -phase, with a weak indication of the monoclinic  $\alpha$ -phase at  $2\theta = 38.7^\circ$  [12]. While the possibility of  $\beta$ -phase cannot be entirely ruled out from the XRD pattern alone, the predominant  $\alpha$ -phase is evident, which can also be influenced by film preparation conditions [10, 13]. Observations from the XRD patterns of blend samples reveal a decrease in amorphous nature with increasing weight percentage of PVDF-HFP in the blend. As the PVDF-HFP content increases, the halo nature of the main peak of PVB transitions into a narrower peak with new  $2\theta$  positions. At higher weight percentages of PVDF-HFP, the blend samples exhibit a semi-crystalline nature. Various parameters obtained from the XRD patterns of blend samples, such as interplanar distance, crystallite size, and order of crystallinity [14], are summarized in Table 1. The table illustrates that particle size and crystallinity increase, and the position of the peak decreases in blends as the weight percentage of PVDF-HFP increases. This indicates that interatomic interactions occur, initiating the formation of crystalline regions starting from 10 wt% of PVDF-HFP. The formation of the blend appears compatible within this composition range.

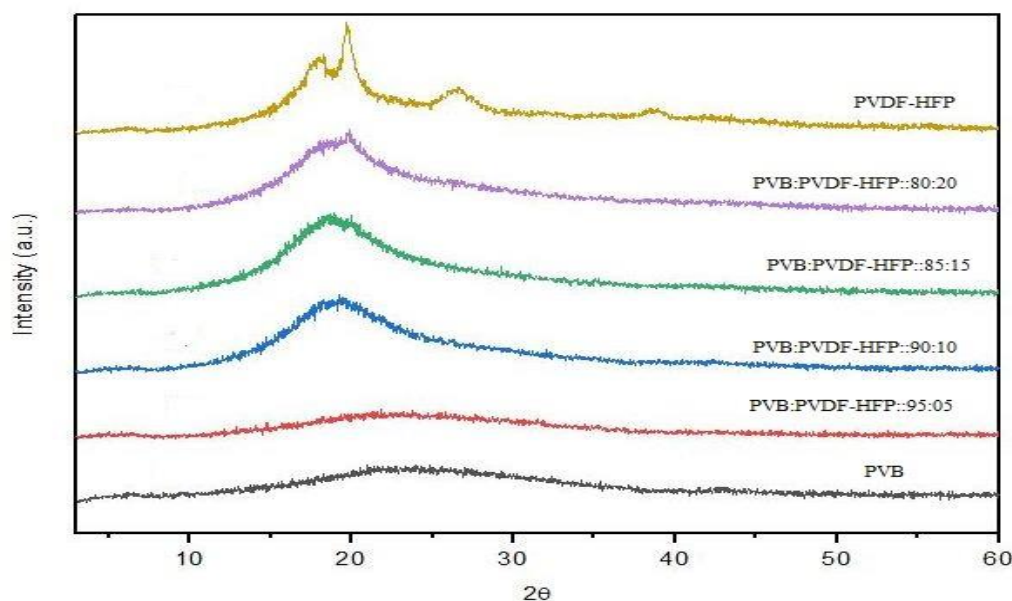


**Figure 2:** XRD Pattern of PVB, PVDF-HFP and their blends i.e. PVB: PVDF-HFP:: 95:05;90:10;85:15 and 80:20

**Table 1. Calculated value of Interplanar spacing, crystallite size and crystallinity index for pure PVB, pure PVDF-HFP and their blends from XRD pattern.**

Blend of PVB:PVDF-HFP	Peak at 2θ	Interplanar Distance (d) in Å	Crystallite Size (D) in Å	Crystallinity Index (Crl) (%)
100:0	23.94	3.720	5.18	-
95:05	22.82	3.893	5.21	-
90:10	19.2	4.618	14.38	23
85:15	18.74	4.731	17.57	25
80:20	19.86	4.466	18.67	27
0:100	18.18	4.93	17.29	44
	19.68	4.49	159.47	

### 3.3DSC

The DSC characterization in this study was employed to analyze the glass transition temperature ( $T_g$ ) and the miscibility of polymer blends. Figure 3 displays the DSC thermograms of both pure polymers and blend samples. A detailed examination of these thermograms reveals a single  $T_g$  for both the pure polymers and the blend samples. The presence of a single  $T_g$  in the blend samples, positioned between the  $T_g$  values of the individual polymers and notably below the  $T_g$  of PVB, indicates the miscibility of the two polymers within this composition range or the formation of a compatible blend [15].

The shifting of  $T_g$  towards lower temperatures is observed with an increase in the weight percentage of PVDF-HFP in the blend. This shift occurs because the nucleation and growth of PVDF-HFP crystals increase with higher concentrations in the blend. This growth decreases the interactions among adjacent polymer chain segments, thereby enhancing the micro-brownian motion and polymer chain mobility of PVB in the blend. This behavior suggests that PVDF-HFP acts as a plasticizer in the blend, resulting in the observed lowering of  $T_g$  with increasing PVDF-HFP content [16].

The glass transition temperature and crystallinity of PVB vary widely depending on the vinyl alcohol percentage [2]. In this study, the  $T_g$  of pure PVB was found to be 73.65°C, confirming its amorphous nature. This  $T_g$  value also indicates that the DSC thermogram did not exhibit any melting or crystalline peak [17]. However, in the blend samples, the DSC thermogram shows a broad transition and small crystalline peaks in samples with higher PVDF-HFP content, suggesting the presence of heterogeneous phases at a microscale in these blends. The broadening of the transition in miscible blends often indicates miscibility without strong specific interactions between the blend components [15].

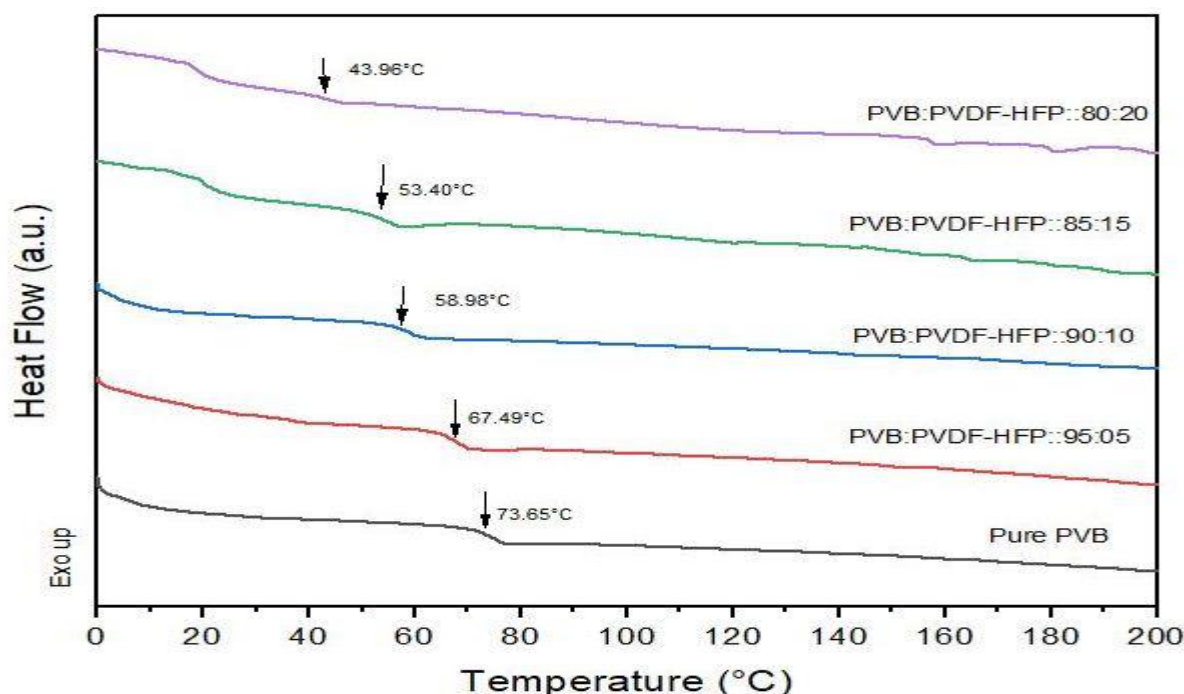


**Figure 3: DSC thermograms of pure PVB and blends i.e. PVB: PVDF-HFP:: 95:05;90:10;85:15 and 80:20**

The Gordon-Taylor equation is utilized in our study for quantitative analysis of  $T_g$  with composition dependence [18]. This equation is selected among various models for  $T_g$  prediction in blend systems, under the assumption that there are no strong interactions present within the blend [19-20]. The Gordon-Taylor equation is represented as

$$T_g = \frac{xT_{g1} + k(1-x)T_{g2}}{x + k(1-x)}$$

When  $K=1$

$$T_g = xT_{g1} + (1 - x)T_{g2}$$

Where  $x$  is the wt% of the component with lower  $T_g$ , which can be plasticizer,  $T_{g1}$  and  $T_{g2}$  are the Glass transition temperature of lower and higher  $T_g$ 's of participating polymer and  $k$  is curve fitting parameter, indicating the nature of miscibility.

Figure 4 illustrates the variation of theoretical and experimental  $T_g$  values with increasing weight percentage of PVDF-HFP. The Gordon-Taylor equation with a coefficient  $K=6$  shows a good fit with the experimental values obtained from DSC. A negative deviation from  $K=1$  indicates adherence to the general rule of mixture, with values of  $K<1$  suggesting weak interactions within the blend samples. This theoretical model further supports the observation that the interactions between PVB and PVDF-HFP are not very strong within this composition range [19-20].

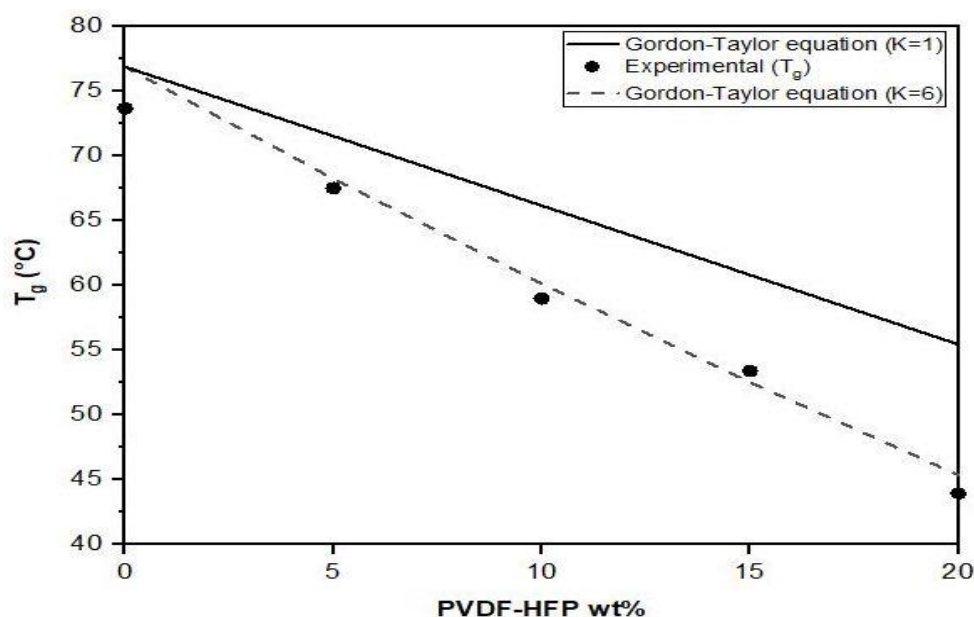


Figure 4: Variation of theoretical and experimental  $T_g$  with increase wt% of PVDF-HFP

### 3.4 Micro-Hardness

Vickers microhardness numbers (Hv) were calculated for pure PVB, pure PVDF-HFP, and their blend samples at different weight percentages (PVB:PVDF-HFP::95:05; 90:10; 85:15; and 80:20) using various loads ranging from 20 to 80 g. Figure 5 illustrates the variation of microhardness with respect to load for the pure polymers and their blend samples. From Figure 5, it is evident that the microhardness number increases rapidly with increasing load at low loads and then slows down at higher loads, eventually reaching a saturated value at loads beyond 50 g. These saturated values indicate the onset of permanent deformation in the samples due to chain-chain slipping between homopolymer or copolymer chain segments after reaching a particular load limit. This behavior can be attributed to the strain hardening phenomenon observed in polymers [21-22].

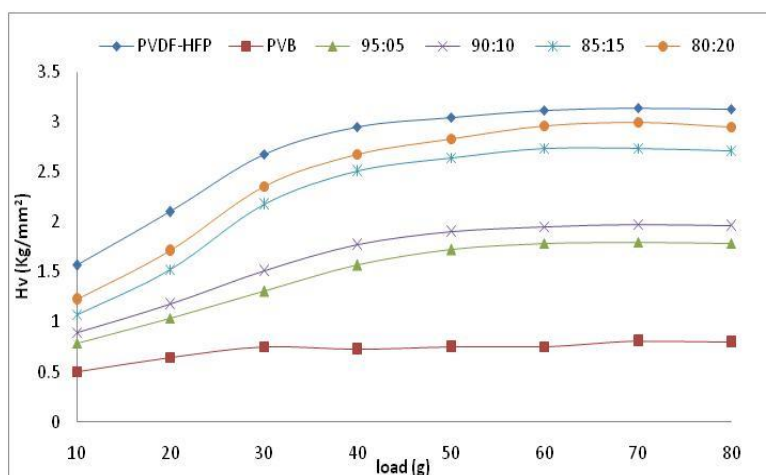


Figure 5: Variation of micro hardness number (Hv) with respect to load for pure PVB, pure PVDF-HFP and their blend samples i.e. PVB: PVDF-HFP:: 95:05; 90:10; 85:15 and 80:20.



The variation of microhardness number exhibits a curvilinear relationship with respect to load across all investigated samples. This characteristic curve can be elucidated by Amontons' theory [23], which correlates microhardness with frictional force. According to this theory, the coefficient of friction decreases as the load increases, while the frictional force increases linearly with the load. As a result, the variation of Hv with load follows a curvilinear pattern, indicating that the microhardness does not increase linearly with load. This behavior is indicative of the small stress behavior attributed to Newtonian resistance pressure [24-25].

Figure 6 depicts the plot of Hv (Vickers microhardness) versus weight percentage of PVDF-HFP in blend samples at various constant load values (20, 40, 60, and 80 g). The Hv value is highest for the pure PVDF-HFP sample and lowest for the pure PVB sample. The curves for blend samples fall between those of the two pure polymers.

The Hv values tend to increase with increasing PVDF-HFP content up to 5 wt%, and then there is no significant increase up to 10 wt%. Beyond 10 wt%, the Hv value again increases up to 15 wt%, followed by a slight decrease at 20 wt%. This trend suggests that increasing the content of PVDF-HFP in the blend enhances its stiffness and toughness, as indicated by the increase in Hv. This improvement can be attributed to interactions between the polar units of PVB and PVDF-HFP, as well as cooperative rearrangement of the amorphous components in the blend [26-27].

In this investigation, IR and XRD studies also confirm that increasing PVDF-HFP content increases crystallinity in the blend, which correlates with the observed increase in microhardness value. However, DSC studies reveal a decrease in Tg values with increasing PVDF-HFP content in the blend, suggesting that PVDF-HFP acts as a plasticizer, resulting in a softening effect on the blend.

It is noteworthy that pure PVDF-HFP is a semi-crystalline polymer with a Tg of approximately -30°C. Polymers characterized by Tg values below room temperature typically do not exhibit high microhardness due to significant deviation from typical deformation mechanisms [28-29]. However, this apparent contradiction has been discussed by various authors [30-31], suggesting that even small amounts of low molecular weight and low Tg polymers can increase microhardness and cause a decrease in Tg in amorphous-crystalline blends.

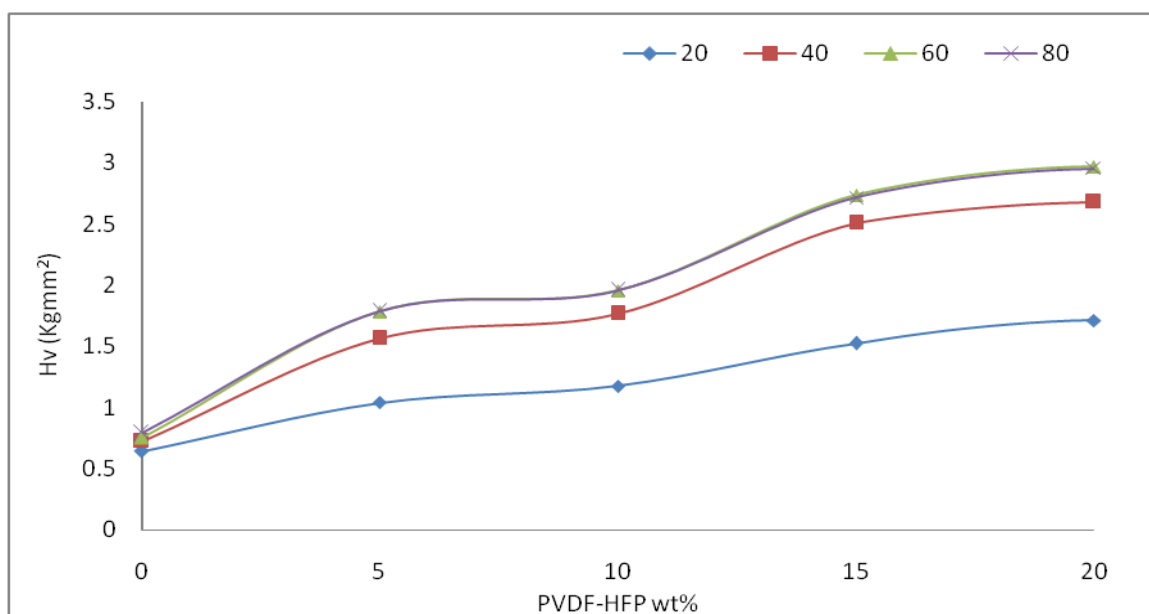


Figure 6: Variation of Hv with increasing wt % of PVDF-HFP in blend samples.

#### 4. CONCLUSION

The XRD studies indicate that the prepared blend samples exhibit higher crystallinity compared to pure PVB, with crystallization initiating around 10 wt% PVDF-HFP and increasing further with higher PVDF-HFP content. In both FTIR and XRD analyses, peak shifts confirm that PVDF-HFP is predominantly in its  $\alpha$ -phase within the blend samples, suggesting some level of interaction between the polymers, albeit not highly significant. The results from XRD correlate well with those from FTIR.

DSC thermograms indicate the miscibility of the blends due to the presence of a single Tg, with a decrease in Tg values as the weight percentage of PVDF-HFP increases, indicating that PVDF-HFP may act as a plasticizer in the blend. However, theoretical calculations using the Gordon-Taylor equation suggest that while interactions between the polymers occur, they are not very strong.

Microhardness measurements show that blend samples have lower microhardness compared to pure PVDF-HFP but higher than pure PVB. This increase in microhardness with increasing PVDF-HFP content suggests homogeneity and compatibility within the studied composition range of the blends. From a strength perspective, this property could be advantageous for various applications. In general, different

characterizations in this investigation indicate that the prepared blend exhibits compatibility within the selected composition range.

## REFERENCES

1. Utracki LA, editor. *Polymer Blends Handbook* [Internet]. Dordrecht: Springer Netherlands; 2003 [cited 2019 Aug 9]. Available from: <http://link.springer.com/10.1007/0-306-48244-4>
2. Olabisi, O. and Adewale, K. Eds. *Handbook of thermoplastics*. Boca Raton, Florida: CRC press 2016. <https://doi.org/10.1201/b19190>
3. Aravindan V, Vickraman P, Kumar TP. Polyvinylidene fluoride–hexafluoropropylene (PVdF–HFP)-based composite polymer electrolyte containing LiPF<sub>3</sub> (CF<sub>3</sub>CF<sub>2</sub>)<sub>3</sub>. *J Non Cryst Solids*. 2008 Jul 1; 354(29):3451–7. <https://doi.org/10.1016/j.jnoncrysol.2008.03.009>
4. Dawande K, Patel S, Bajpai R, Keller JM. Dielectric relaxation behaviour of (poly (vinyl formal)) (PVFO) and polyvinylidene fluoride (PVDF) blends. In: *AIP Conference Proceedings* [Internet]. AIP Publishing LLC; 2018 [cited 2019 Aug 5]. p. 050034. Available from: <http://aip.scitation.org/doi/abs/10.1063/1.5032689>
5. Kamalova DI, Naumova SN, Abdrazakova LR. Binary Polymer Systems Based on Polyvinylbutyral: FTIR Spectra, Conformational Dynamics, and Free Volume. *Bull Russ Acad Sci Phys* [Internet]. 2018 Aug 1 [cited 2024 Jun 16];82(8):1057–61. Available from: <https://link.springer.com/article/10.3103/S106287381808018X>
6. Shalu, Chaurasia SK, Singh RK, Chandra S. Thermal stability, complexing behavior, and ionic transport of polymeric gel membranes based on polymer PVdF-HFP and ionic liquid, [BMIM][BF<sub>4</sub>]. *J Phys Chem B* [Internet]. 2013 Jan 24 [cited 2023 Aug 24];117(3):897–906. Available from: <https://pubs.acs.org/doi/abs/10.1021/jp307694q>
7. Luan W, Sun L, Zeng Z, Xue W. Optimization of a polyvinyl butyral synthesis process based on response surface methodology and artificial neural network. *RSC Adv* [Internet]. 2023 Mar 1 [cited 2023 Sep 13];13(11):7682–93. Available from: <https://pubs.rsc.org/en/content/articlehtml/2023/ra/d2ra08099k>
8. Riaz U, Ashraf SM. Characterization of Polymer Blends with FTIR Spectroscopy. In: Thomas S, Grohens Y, Jyotishkumar P, editors. *Characterization of Polymer Blends*. 1st ed. Weinheim: John Wiley & Sons 2014 : P. 625-678 <https://doi.org/10.1002/9783527645602.ch20>
9. Du CH, Zhu BK, Xu YY. The effects of quenching on the phase structure of vinylidene fluoride segments in PVDF-HFP copolymer and PVDF-HFP/PMMA blends. *J Mater Sci* 2006 412 [Internet]. 2006 Jan 1 [cited 2021 Dec 8];41(2):417–21. Available from: <https://link.springer.com/article/10.1007/s10853-005-2182-6>
10. Salimi A, Yousefi AA. FTIR studies of  $\beta$ -phase crystal formation in stretched PVDF films. *Polym Test*. 2003 Sep 1;22(6):699–704.
11. Hajian M, Reisi MR, Koohmareh GA, Jam ARZ. Preparation and characterization of polyvinylbutyral/Graphene nanocomposite. *J Polym Res* [Internet]. 2012 Oct 1 [cited 2024 Jun 17];19(10):1–7. Available from: <https://link.springer.com/article/10.1007/s10965-012-9966-6>
12. Cai X, Lei T, Sun D, Lin L. A critical analysis of the  $\alpha$ ,  $\beta$  and  $\gamma$  phases in poly(vinylidene fluoride) using FTIR. *RSC Adv* [Internet]. 2017 Mar 6 [cited 2019 Jul 29];7(25):15382–9. Available from: <http://xlink.rsc.org/?DOI=C7RA01267E>
13. Boccaccio T, Bottino A, Capannelli G, Piaggio P. Characterization of PVDF membranes by vibrational spectroscopy. *J Memb Sci*. 2002 Dec 15;210(2):315–29.
14. Patel AK, Bajpai R, Keller JM, Kumari B, Vatsal V, Saha A. Structural, morphological and micromechanical studies on fly ash reinforced PMMA composites. *Microsyst Technol* [Internet]. 2011 Dec 1 [cited 2020 Aug 15];17(12):1755–62. Available from: <https://link.springer.com/article/10.1007/s00542-011-1356-1>
15. Zhang G, Zhang J, Wang S, Shen D. Miscibility and phase structure of binary blends of polylactide and poly(methyl methacrylate). *J Polym Sci Part B Polym Phys* [Internet]. 2002 Jan 1 [cited 2020 Jun 27];41(1):23–30. Available from: <https://www.onlinelibrary.wiley.com/doi/full/10.1002/polb.10353>
16. Thirtha V, Lehman R, Nosker T. Morphological effects on glass transition behavior in selected immiscible blends of amorphous and semicrystalline polymers. *Polymer (Guildf)*. 2006 Jul 12;47(15):5392–401.
17. Han D, Guo Z, Chen S, Xiao M, Peng X, Wang S, et al. Enhanced Properties of Biodegradable Poly(Propylene Carbonate)/Polyvinyl Formal Blends by Melting Compounding. *Polym* 2018, Vol 10, Page 771 [Internet]. 2018 Jul 13 [cited 2021 Sep 25];10(7):771. Available from: <https://www.mdpi.com/2073-4360/10/7/771/htm>
18. Gordon JM, Rouse GB, Gibbs JH, Risen WM. The composition dependence of glass transition properties. *J Chem Phys* [Internet]. 1977 Jun 26 [cited 2020 Jun 27];66(11):4971–6. Available from: <http://aip.scitation.org/doi/10.1063/1.433798>
19. Huang J, Guo Q. Compatibility of poly(N-vinyl-2-pyrrolidone) with poly(vinyl formal) and poly(styrene-co-acrylonitrile). *Die Makromol Chemie, Rapid Commun* [Internet]. 1990 Dec 1 [cited 2020 Jun 27];11(12):613–6. Available from: <http://doi.wiley.com/10.1002/marc.1990.030111204>

20. Fan W, Zheng S. Miscibility and crystallization behavior in blends of poly(methyl methacrylate) and poly(vinylidene fluoride): Effect of star-like topology of poly(methyl methacrylate) chain. *J Polym Sci Part B Polym Phys* [Internet]. 2007 Sep 15 [cited 2020 Jun 27]; 45(18):2580–93. Available from: <http://doi.wiley.com/10.1002/polb.21264>
21. Lopez J. Microhardness testing of plastics: Literature review. *Polym Test* [Internet]. 1993 Jan 1 [cited 2019 Aug 20];12(5):437–58. Available from: <https://www.sciencedirect.com/science/article/pii/0142941893900161>
22. Mishra V, Bajpai R, Datt SC. Radiation induced effects on the microhardness measurements of poly(methyl methacrylate): poly (vinylidene fluoride) polyblends. *Polym Test* [Internet]. 1994 Jan 1 [cited 2019 Aug 20];13(5):435–40. Available from: <https://www.sciencedirect.com/science/article/pii/0142941894900523>
23. Stamm M, Polymer surfaces and interfaces. Characterization, Modification and Applications. 1<sup>st</sup> ed. Springer: Berlin, Germany: 2008. <https://doi.org/10.1007/978-3-540-73865-7>
24. Parashar P, Bajpai R, Keller JM, Datt SC. Microhardness measurement of polypropylene, poly(ethylene terephthalate) and poly(tetra-fluoroethylene). *Makromol Chemie Macromol Symp* [Internet]. 1988 Jul 1 [cited 2019 Aug 20];20–21(1):465–74. Available from: <http://doi.wiley.com/10.1002/masy.19880200149>
25. Dubey V, Bajpai R, Parashar P, Datt SC. Studies of the microhardness of glass fibre reinforced polymer (GFRP). *Polym Test* [Internet]. 1992 Jan 1 [cited 2019 Aug 20];11(3):225–31. Available from: <https://www.sciencedirect.com/science/article/pii/014294189290053E>
26. Suresh G, Jatav S, Geethu PM, Rephung Y, Ramachandra Rao MS, Satapathy DK. Poly(vinylidene fluoride)-Formvar blends: Dielectric, miscibility and mechanical studies. *J Phys D Appl Phys* [Internet]. 2018 Jan 24 [cited 2021 Jan 9];51(6):065604. Available from: <https://iopscience.iop.org/article/10.1088/1361-6463/aaa39c>
27. Zouai F, Benabid FZ, Bouhelal S, Cagiao ME, Benachour D, Baltá Calleja FJ. Nanostructure and morphology of poly(vinylidene fluoride)/polymethyl (methacrylate)/clay nanocomposites: correlation to micromechanical properties. *J Mater Sci* [Internet]. 2017 Apr 1 [cited 2021 Jan 9];52(8):4345–55. Available from: <https://link.springer.com/article/10.1007/s10853-016-0664-3>
28. Flores A, Ania F, Baltá-Calleja FJ. From the glassy state to ordered polymer structures: A microhardness study. Vol. 50, *Polymer*. Elsevier BV; 2009. p. 729–46. <https://doi.org/10.1016/j.polymer.2008.11.037>
29. Baltá Calleja FJ, Rueda DR, Boyanova M, Fakirov S. On the Relationship between Microhardness and Crystal Perfection of Chain-Extended Polyethylene. *J Macromol Sci - Phys* [Internet]. 2003 Nov [cited 2020 Jun 28];42 B(6):1293–9. Available from: <https://www.tandfonline.com/doi/abs/10.1081/MB-120024821>
30. Bajpai R, Mishra V, Agrawal P, Datt SC. Surface modification on PMMA: PVDF polyblend: Hardening under chemical environment. *Bull Mater Sci* [Internet]. 2002 [cited 2020 Jun 28];25(1):21–3. Available from: <https://link.springer.com/article/10.1007/BF02704589>
31. Riggleman RA, Douglas JF, De Pablo JJ. Antiplasticization and the elastic properties of glass-forming polymer liquids. *Soft Matter* [Internet]. 2010 Jan 8 [cited 2021 Jan 6];6(2):292–304. Available from: <https://pubs.rsc.org/en/content/articlehtml/2010/sm/b915592a>

DOI: <https://doi.org/10.15379/ijmst.v10i2.3742>

This is an open access article licensed under the terms of the Creative Commons Attribution Non-Commercial License (<http://creativecommons.org/licenses/by-nc/3.0/>), which permits unrestricted, non-commercial use, distribution and reproduction in any medium, provided the work is properly cited.